

Penalized Wall Function Method for Turbulent Flow Modeling

Natalia S. Zhdanova¹ , Oleg V. Vasilyev¹ 

© The Authors 2022. This paper is published with open access at SuperFri.org

A novel penalized wall function method for simulations of wall-bounded compressible turbulent flows is proposed. The new approach is based on the Reynolds-averaged Navier–Stokes (RANS) equations to model the outer region of the turbulent boundary layer, while the inner part is approximated by the equilibrium wall function model. The differential formulation to match the external and the wall function solutions is reformulated in a form of the generalized characteristic-based volume penalization method to model the transfer of the shear stress from the outer region of the boundary layer to the wall and to impose the wall-stress boundary conditions on the RANS solution. The exchange location is specified implicitly through a localized source term in the boundary layer equation, written as a function of the normalized distance from the wall. The wall-stress condition is determined by solving an auxiliary equation for the wall-stress, ensuring the correct matching of the RANS and the wall function solutions at the exchange layer. The proposed method noticeably reduces the near-wall mesh resolution requirements without significant modification of the RANS solver and removes the ill-defined explicit matching procedure, commonly used by traditional wall function-based methods. The penalized wall function approach is implemented using the vertex-centered control volume method on unstructured computational grids. The effectiveness of the developed penalized wall function method is demonstrated for two-dimensional bump-in-channel flow for the Spalart–Allmaras turbulence model.

Keywords: turbulence modeling, wall function, wall-bounded compressible turbulent flow, volume penalization.

Introduction

Accurate modeling of turbulent flows of engineering interest remains to be one of the major challenges of computational fluid dynamics. Due to prohibitively expensive computational cost of the direct numerical simulations (DNS) of large Reynolds number turbulent flows [24], a number of lower fidelity eddy-resolving approaches are currently actively being pursued. These methods are based either on the Reynolds-averaged Navier–Stokes (RANS) equations [14, 16, 31, 35] or on hybrid approaches [15, 36], in which the flow in the near-wall region is simulated using RANS-type models, while in regions far from the walls the Large Eddy Simulation (LES) method is used. The hybrid class of methods also includes detached eddy simulation (DES) methods [30, 32, 33] with a smooth transition from RANS to LES solutions.

Despite relatively moderate near-wall resolution requirements of RANS, hybrid RANS-LES, and DES approaches, these requirements are still significant and impose strict limitations on the computational resources, considerably increase the computation time, and complicate the computational grid construction.

Mesh resolution restrictions can be substantially reduced if the boundary solution is approximated by a wall function and only external RANS solution is simulated [11, 27]. This can be achieved by replacing no-slip wall boundary conditions with off-the-wall boundary conditions at the exchange location away from the wall. Alternatively a weak wall function formulation can be used to transfer the shear stress from the outer region of the boundary layer to the wall and to impose the wall-stress boundary conditions on the RANS solution [5, 13]. A weak wall function formulation is more preferable from the computational point of view due to its flexibility, but it does not guarantee an exact correspondence of the boundary layer displacement thicknesses,

¹Keldysh Institute of Applied Mathematics, Russian Academy of Sciences, Moscow, Russian Federation

mainly due to approximate nature of the solution in the near-wall region with the slip velocity and turbulent viscosity extrapolated from the outer region of the solution, which results in a decrease of the displacement thickness compared to the RANS solution with no-slip boundary conditions.

In traditional wall function approaches [25] the boundary conditions are determined by solving nonlinear equations at the matching (exchange) location, which is not known a priori and is implicitly defined by the normalized distance from the wall, which, in turn, is a function of the wall shear stress. For this purpose, the solution at the exchange location, is interpolated from the nearest computational mesh points [7]. It should be noted that wall functions can be used in conjunction with immersed boundary methods, where additional constraints at the immersed mesh points are imposed to ensure the boundary conditions on the surface of the obstacle [6, 10, 12].

The main idea of the proposed approach, hereinafter referred to as the *Penalized Wall Function* (PWF) method, is to replace the nonlinear algebraic matching condition between the external and wall function solutions by a differential formulation based on a generalized characteristic-based volume penalization method [8, 19] to transfer the shear stress from the outer region of the boundary layer to the wall, while specifying exchange locations implicitly through the localized source term in the boundary layer equation, written as a function of the normalized distance from the wall. Such an approach, makes it possible to completely eliminate the need to explicitly find the exchange location, and, more importantly, reduces the system of partial differential equations with nonlinear algebraic constraints to a system of partial differential equations with differential feedback loop provided by characteristic penalty functions. The latter property makes it feasible to generalize the approach to problems with flow separation based on differential equilibrium [7, 20] and non-equilibrium [21, 26] wall functions. In general, the developed approach noticeably reduces the near-wall mesh resolution requirements without significant modification of the RANS solver. Note that the developed PWF method should be distinguished from hybrid approaches utilizing immersed boundary methods to set boundary conditions on the surface of the obstacles [6, 10], since it uses characteristic-based volume penalization to match external and wall function solutions. Furthermore, the PWF method can also be generalized for complex geometry flows, based on the already developed volume penalization methods [2, 8, 19, 22, 23, 37].

The rest of the paper is organized as follows. In Section 1 the governing equations of the numerical simulations, including the Favre-averaged Navier–Stokes equations for compressible flows and the evolution equations for turbulence models are introduced. The penalized wall function method for turbulent flow modeling is formulated in Section 2. The numerical method used to implement the PWF approach is briefly described in Section 3. The 2D bump-in-channel flow configuration and the corresponding simulation results using the PWF method are presented and discussed in Section 4. Concluding remarks are given in Section 4.1.

1. Governing Equations

1.1. Favre-averaged Navier–Stokes Equations

Compressible RANS equations are formulated in terms of Reynolds-averaged and Favre-averaged dependent variables. Denoting Reynolds-averaging and Favre-averaging operations as $\langle \phi \rangle$ and $\{\phi\} = \langle \rho \phi \rangle / \langle \rho \rangle$, respectively, where ϕ stands for a generic physical variable, the method involves Reynolds-averaged density $\langle \rho \rangle$ and pressure $\langle p \rangle$, together with Favre-averaged veloc-

ity $\{u_i\}$, temperature $\{T\}$, and total energy per unit mass $\{e\}$. For the sake of clarity, the corresponding operator symbols hereafter are omitted in the notations of Reynolds/Favre-averaged primitive variables and simple symbols ρ , p , u_i , T and e are used hereafter to denote the Reynolds-averaged density, pressure, and Favre-averaged velocity, temperature, and total energy per unit mass. Therefore, the Favre-averaged Navier–Stokes equations for the conservation of mass, momentum, and energy in compressible flows for calorically perfect gas after incorporation of modeled turbulent terms using the Boussinesq eddy viscosity, eddy-conductivity, and constant turbulent Prandtl number assumptions can be written in the following general form:

$$\frac{\partial \rho}{\partial t} + \frac{\partial(\rho u_j)}{\partial x_j} = 0, \quad (1)$$

$$\frac{\partial \rho u_i}{\partial t} + \frac{\partial}{\partial x_j} (\rho u_i u_j) = -\frac{\partial p}{\partial x_i} + \frac{\partial \hat{\tau}_{ij}}{\partial x_j}, \quad (2)$$

$$\frac{\partial \rho e}{\partial t} + \frac{\partial}{\partial x_j} [(\rho e + p) u_j] = \frac{\partial}{\partial x_j} [u_i \hat{\tau}_{ij} - q_j], \quad (3)$$

where

$$p = \rho R T, \quad (4)$$

$$e = \frac{1}{2} u_i u_i + \frac{p}{\rho(\gamma - 1)}, \quad (5)$$

$$q_j = -c_p \left(\frac{\mu}{Pr_L} + \frac{\mu_T}{Pr_T} \right) \frac{\partial T}{\partial x_j}, \quad (6)$$

$$\hat{\tau}_{ij} = 2\mu \tilde{S}_{ij} + \tau_{ij},$$

$$\tau_{ij} = 2\mu_T \tilde{S}_{ij}, \quad (7)$$

$$\tilde{S}_{ij} = \text{dev}(S_{ij}) = S_{ij} - \frac{1}{3} \frac{\partial u_k}{\partial x_k} \delta_{ij},$$

$$S_{ij} = \frac{1}{2} \left(\frac{\partial u_i}{\partial x_j} + \frac{\partial u_j}{\partial x_i} \right).$$

In the equations above, the parameter R stands for the gas constant, while c_v and c_p are the specific heat constants at constant volume and pressure, respectively. The specific heat ratio $\gamma = \frac{c_p}{c_v} \equiv 1.4$ for diatomic gases is assumed. The term q_j is the sum of both the laminar and the modeled turbulent heat flux vectors, with $Pr_L = 0.72$ and $Pr_T = 0.9$ being the laminar and the turbulent Prandtl numbers, respectively. The turbulent eddy viscosity is denoted by μ_T , which is unknown and needs turbulence models for closure. The term $\hat{\tau}_{ij}$ is the sum of the molecular and the Reynolds stress tensors, while τ_{ij} is the Reynolds stress tensor, S_{ij} is the mean strain-rate tensor, and \tilde{S}_{ij} is the deviatoric part of S_{ij} . For simplicity of consideration, constant dynamic molecular viscosity μ is assumed, which is a good approximation for low Mach number flows considered in this paper.

1.2. Turbulence Model Equations

Without loss of generality, the Spalart–Allmaras (S-A) turbulence model [31] is used to illustrate the developed penalized wall function approach. The S-A model is widely used as a turbulence model closure for the equations (6) and (7), including high-velocity flows with a significant effect of compressibility [4].

The standard Spalart–Allmaras model [31] in terms of $\rho\tilde{\nu}$ can be written as follows:

$$\begin{aligned} \frac{\partial \rho\tilde{\nu}}{\partial t} + \frac{\partial}{\partial x_j} (\rho\tilde{\nu}u_j) &= c_{b1}(1 - f_{t2})\tilde{S}\rho\tilde{\nu} - \left[c_{w1}f_w - \frac{c_{b1}}{\kappa^2}f_{t2} \right] \rho \left(\frac{\tilde{\nu}}{\delta} \right)^2 \\ &+ \frac{\partial}{\partial x_j} \left[\left(\frac{\mu}{\sigma} + \frac{\rho\tilde{\nu}}{\sigma} \right) \frac{\partial \tilde{\nu}}{\partial x_j} \right] - \left(\frac{\mu}{\sigma\rho} + \frac{\tilde{\nu}}{\sigma} \right) \frac{\partial \rho}{\partial x_j} \frac{\partial \tilde{\nu}}{\partial x_j} + c_{b2} \frac{\rho}{\sigma} \frac{\partial \tilde{\nu}}{\partial x_j} \frac{\partial \tilde{\nu}}{\partial x_j}, \end{aligned} \quad (8)$$

where the eddy viscosity is computed by

$$\mu_T = \rho\tilde{\nu}f_{v1}, \quad (9)$$

and auxiliary variables are defined as:

$$\begin{aligned} f_{v1} &= \frac{\chi^3}{\chi^3 + c_{v1}^3}, \\ \chi &= \tilde{\nu}/\nu, \\ \tilde{S} &= \max \left[0.3\sqrt{2\Omega_{ij}\Omega_{ij}}, \sqrt{2\Omega_{ij}\Omega_{ij}} + \frac{\tilde{\nu}}{\kappa^2\delta^2}f_{v2} \right], \\ \Omega_{ij} &= \frac{1}{2} \left(\frac{\partial u_i}{\partial x_j} - \frac{\partial u_j}{\partial x_i} \right), \\ f_{v2} &= 1 - \frac{\chi}{1 + \chi f_{v1}}, \\ f_w &= g \left[\frac{1 + c_{w3}^6}{g^6 + c_{w3}^6} \right]^{1/6}, \\ g &= r + c_{w2}(r^6 - r), \\ r &= \min \left[\frac{\tilde{\nu}}{\tilde{S}\kappa^2\delta^2}, 10 \right], \\ f_{t2} &= c_{t3} \exp(-c_{t4}\chi^2), \end{aligned} \quad (10)$$

where ν is kinematic molecular viscosity, $\delta(\mathbf{x})$ is the distance from the field point to the nearest wall, and to improve the stability of calculations the variable \tilde{S} is bounded from below by the quantity $0.3\sqrt{2\Omega_{ij}\Omega_{ij}}$. The constant coefficients are prescribed as $c_{b1} = 0.1355$, $c_{b2} = 0.622$, $\sigma = 2/3$, $\kappa = 0.41$, $c_{w2} = 0.3$, $c_{w3} = 2$, $c_{v1} = 7.1$, $c_{w1} = \frac{c_{b1}}{\kappa} + \frac{1+c_{b2}}{\sigma}$. Note that this “standard” version of the S-A model does not have the trip term “ f_{t1} ” and, hence, it is argued that f_{t2} is not necessary, i.e., $c_{t3} = 0$ is assumed.

The following boundary condition on the wall surface

$$\tilde{\nu} = 0 \quad (12)$$

is used for consistency. When modeling external flows the constant turbulent viscosity $\tilde{\nu} = 3\nu_\infty$ is assumed at the inflow boundary.

2. Penalized Wall Function Method

The considerably lower computational cost of eddy-resolving approaches compared to DNS or LES, makes RANS-based methods to be a method of choice for high Reynolds number turbulent flow simulations in aerospace industry. However, despite relatively moderate near-wall resolution requirements of RANS [14, 16, 31, 35], hybrid RANS-LES [15, 36], and DES [30, 32, 33] approaches, the direct resolution of flow structures of the RANS equations (1)–(3), (8) results in a

considerable computational cost associated with a large number of mesh points in the near-wall region. Mesh resolution restrictions can be substantially reduced if instead of resolving the solution in the vicinity of the wall, it is approximated by a wall function and only external RANS solution is obtained [11, 27]. This can be achieved by replacing no-slip boundary conditions on the wall with the matching conditions between the wall function and the outer turbulent boundary layer solutions:

$$u_{\parallel}(\mathbf{x})\Big|_{\delta(\mathbf{x})=\frac{\nu}{u_{\tau}}\delta_{\text{EL}}^+} = u_{\tau}f(\delta_{\text{EL}}^+), \quad (13)$$

where the matching (exchange) location is determined from the following condition:

$$\delta(\mathbf{x}) = \frac{\nu}{u_{\tau}}\delta_{\text{EL}}^+, \quad (14)$$

$u_{\parallel}(\mathbf{x})$ is the velocity component parallel to the surface at point \mathbf{x} , \tilde{x} and \tilde{y} are generalized coordinates along and normal to the wall, $\tilde{y}^+ = u_{\tau}\tilde{y}/\nu$ is the normalized coordinate, $u_{\tau} = (\tau_w/\rho)^{1/2}$ is the friction velocity, τ_w is the wall stress, δ_{EL}^+ is the normalized distance to the exchange location, and $f(\tilde{y}^+)$ is the wall function, defined as a function of the distance from the wall, normalized by the viscous length scale. Note that Eq. (14) can be viewed as a non-linear algebraic equation for determining the exchange location for a given coordinate \tilde{x} on the wall. For the sake of simplicity, let us start by formulating the method for two-dimensional flows. The generalization of the method to three-dimensional flows will be provided at the end of the section.

For a given external velocity field $u_{\parallel}(\mathbf{x})$ and for a given normalized distance δ_{EL}^+ the matching condition (13) is a non-linear algebraic equations for determining u_{τ} . A linear approximation of Eq. (13) for the friction velocity correction δu_{τ} can be written as

$$u_{\parallel}(\mathbf{x})\Big|_{\delta(\mathbf{x})=\frac{\nu}{u_{\tau}}\delta_{\text{EL}}^+} + \frac{\partial u_{\parallel}(\mathbf{x})}{\partial \mathbf{n}}\Big|_{\delta(\mathbf{x})=\frac{\nu}{u_{\tau}}\delta_{\text{EL}}^+} \left(-\frac{\nu\delta_{\text{EL}}^+}{u_{\tau}^2}\delta u_{\tau} \right) \approx u_{\tau}f(\delta_{\text{EL}}^+) + \delta u_{\tau}f(\delta_{\text{EL}}^+), \quad (15)$$

where the normal \mathbf{n} is defined in terms of the distance function $\delta(\mathbf{x})$: $\mathbf{n} = \nabla\delta(\mathbf{x})$. Note that the second term on the left hand side of Eq. (15) arises due to the change of the distance $\delta(\mathbf{x})$ of the exchange location when u_{τ} changes and δ_{EL}^+ is fixed. The solution of Eq. (15) for the friction velocity correction δu_{τ} is given by

$$\delta u_{\tau} \approx u_{\tau} \frac{u_{\parallel}(\mathbf{x})\Big|_{\delta(\mathbf{x})=\frac{\nu}{u_{\tau}}\delta_{\text{EL}}^+} - u_{\tau}f(\delta_{\text{EL}}^+)}{u_{\tau}f(\delta_{\text{EL}}^+) + \frac{\partial u_{\parallel}(\mathbf{x})}{\partial \mathbf{n}}\Big|_{\delta(\mathbf{x})=\frac{\nu}{u_{\tau}}\delta_{\text{EL}}^+} \delta(\mathbf{x})}. \quad (16)$$

When a strong wall function formulation is used, the friction velocity correction (16) can be used in Newton's method to iteratively obtain the solution of the matching condition (13).

For the weak wall function formulation, the discrete friction velocity correction (16) can be replaced by temporal relaxation of the solution $u_{\tau}(\tilde{x}, t)$ on the time scale η_f at each point of the generalized coordinate \tilde{x} , defined along wall:

$$\frac{\partial u_{\tau}}{\partial t} = \frac{u_{\tau}}{\eta_f} \frac{u_{\parallel}(\mathbf{x})\Big|_{\delta(\tilde{x})=\frac{\nu}{u_{\tau}}\delta_{\text{EL}}^+} - u_{\tau}f(\delta_{\text{EL}}^+)}{u_{\tau}f(\delta_{\text{EL}}^+) + \frac{\partial u_{\parallel}(\mathbf{x})}{\partial \mathbf{n}}\Big|_{\delta(\tilde{x})=\frac{\nu}{u_{\tau}}\delta_{\text{EL}}^+} \delta(\tilde{x})}, \quad (17)$$

where for greater clarity the exchange location, implicitly defined by the equation (14), is explicitly written as $\delta(\tilde{x})$, while the no-slip boundary condition for the velocity \mathbf{u} at the wall is

replaced by the no-penetration condition for the normal velocity component $u_{\perp}(\mathbf{x}) = \mathbf{u} \cdot \mathbf{n}$:

$$u_{\perp}|_{\tilde{y}=0} = 0 \quad (18)$$

and the wall shear stress condition:

$$(\nu + \nu_T) \frac{\partial u_{\parallel}}{\partial \mathbf{n}} \Big|_{\tilde{y}=0} = u_{\tau}^2(\tilde{x}, t). \quad (19)$$

For consistent wall function formulation of the Spalart–Allmaras model, the turbulent viscosity from the outer flow region is transferred to the boundary, which can be easily achieved by replacing the distance function $\delta(\mathbf{x})$ in the Eqs. (8), (10) and (11) by

$$\delta(\mathbf{x}) = \max \left(\delta(\mathbf{x}), \frac{\nu}{u_{\tau}} \delta_{\text{EL}}^+ \right) \quad (20)$$

and changing the boundary condition (12) for turbulent viscosity to

$$\frac{\partial \tilde{\nu}}{\partial \mathbf{n}} \Big|_{\tilde{y}=0} = 0. \quad (21)$$

The equation (13) with an implicit determination of the exchange location $\delta(\tilde{x})$ complicates the solution of the problem, since, in general, exchange locations do not coincide with mesh points and the tangential velocity component u_{\parallel} from the nearest mesh points needs to be interpolated to the exchange location, e.g., see [7]. The problem can be greatly simplified and the need to interpolate the tangential velocity to exchange locations can be completely eliminated by introducing an auxiliary friction velocity field $u_{\tau}(\mathbf{x}, t)$, defined in the entire domain and not only on the wall, and by replacing Eq. (17) for $u_{\tau}(\tilde{x}, t)$ on the wall by the following partial differential equation for the field $u_{\tau}(\mathbf{x}, t)$:

$$\underbrace{\frac{\partial u_{\tau}}{\partial t} - \mathcal{H} \left(\delta_{\text{EL}}^+ - \frac{u_{\tau}}{\nu} \delta(\mathbf{x}) \right) \frac{l_s}{\eta_s} \frac{\partial u_{\tau}}{\partial \mathbf{n}}}_{\text{transfer of } u_{\tau} \text{ to the wall}} = \underbrace{\chi_{\delta} \left(\frac{\delta_{\text{EL}}^+ - \frac{u_{\tau}}{\nu} \delta(\mathbf{x})}{\sigma^+} \right) \frac{u_{\tau}}{\eta_f} \frac{u_{\parallel}(\mathbf{x}) - u_{\tau} f(\delta_{\text{EL}}^+)}{u_{\tau} f(\delta_{\text{EL}}^+) + \frac{\partial u_{\parallel}(\mathbf{x})}{\partial \mathbf{n}} \delta(\mathbf{x})}}_{\text{temporal relaxation of } u_{\tau} \text{ in an exchange layer}} + \underbrace{\nu_n \Delta u_{\tau}}_{\text{smoothing}}, \quad (22)$$

where l_s and η_s are, respectively, the characteristic length and time scales of transferring the solution from the exchange layer to the wall, $\mathcal{H}(\xi)$ is the Heaviside function that disables the transfer of u_{τ} in the outer region of the turbulent boundary layer, $\chi_{\delta}(\xi)$ is a localized exchange layer masking function, for example, the Gaussian function

$$\chi_{\delta}(\xi) = \exp(-\xi^2/2), \quad (23)$$

σ^+ is the normalized thickness of the exchange layer, and $\nu_n \Delta u_{\tau}$ is the numerical diffusion used to smooth out the auxiliary field u_{τ} . Note that in Eq. (22), the matching condition (13) is provided by temporal relaxation term in the spatially localized exchange layer, from which u_{τ} is transferred to the wall for the subsequent use in the boundary condition (19). The second term on the left hand side of Eq. (22) corresponds to the characteristic penalty function [8, 9, 19], which on the time scale η_s transfers the friction velocity to the wall.

In order to improve the convergence of the method in the earlier stages of the transient solution, the term $\frac{\partial u_{\parallel}(\mathbf{x})}{\partial \mathbf{n}}$ in the Eq. (22) can be approximated by differentiating the wall function solution:

$$\frac{\partial u_{\parallel}(\mathbf{x})}{\partial \mathbf{n}} \approx \frac{u_{\tau}^2}{\nu} f' \left(\frac{u_{\tau} \tilde{y}}{\nu} \right). \quad (24)$$

Substituting Eqs. (14) and (24) into Eq. (22) the following stabilized penalized wall function equation can be obtained:

$$\frac{\partial u_{\tau}}{\partial t} - \underbrace{\mathcal{H} \left(\delta_{\text{EL}}^+ - \frac{u_{\tau}}{\nu} \delta(\mathbf{x}) \right) \frac{l_s}{\eta_s} \frac{\partial u_{\tau}}{\partial \mathbf{n}}}_{\text{transfer of } u_{\tau} \text{ to the wall}} = \frac{1}{\eta_f} \chi_{\delta} \underbrace{\left(\frac{\delta_{\text{EL}}^+ - \frac{u_{\tau}}{\nu} \delta(\mathbf{x})}{\sigma^+} \right) \frac{u_{\parallel}(\mathbf{x}) - u_{\tau} f(\delta_{\text{EL}}^+)}{f(\delta_{\text{EL}}^+) + f'(\delta_{\text{EL}}^+) \delta_{\text{EL}}^+}}_{\text{temporal relaxation of } u_{\tau} \text{ in an exchange layer}} + \underbrace{\nu_n \Delta u_{\tau}}_{\text{smoothing}}. \quad (25)$$

The equation (25) is the basis of the penalized wall function method. Note that despite the fact that the developed approach has been demonstrated only in the context of the Spalart–Allmaras model, the PWF method can be used in conjunction with any turbulence model that allows transfer of shear stress from the outer region of the boundary layer to the wall. Note that the choice of the exchange location δ_{EL}^+ can affect the accuracy and efficiency of the simulations. In general the exchange location should be chosen to be outside of the viscous sublayer region to improve the near-wall resolution requirements and below the law-of-the-wake region, which is problem dependent.

For three-dimensional flows, the problem can be rewritten in local two-dimensional coordinates, where the coordinate \tilde{x} along the body surface corresponds to the direction of the tangential velocity component at the corresponding exchange location. In this case, the equation (25) can be used without modification under the assumption that the direction of the wall shear is aligned with the tangential velocity vector at the corresponding exchange location, and the variable $u_{\parallel}(\mathbf{x}) = \|\mathbf{u}_{\parallel}(\mathbf{x})\|$ corresponds to the magnitude of the parallel velocity component $\mathbf{u}_{\parallel}(\mathbf{x}) = \mathbf{u} - (\mathbf{u} \cdot \mathbf{n})\mathbf{n}$. Then the boundary conditions (18) and (19) can be rewritten as follows:

$$\mathbf{u} \cdot \mathbf{n}|_{\tilde{y}=0} = 0 \quad (26)$$

$$(\nu + \nu_{\text{T}}) \frac{\partial \mathbf{u}_{\parallel}}{\partial \mathbf{n}} \Big|_{\tilde{y}=0} = \left(\frac{\mathbf{u}_{\parallel}}{u_{\parallel}} \Big|_{\tilde{y}=0} \right) u_{\tau}^2(\tilde{x}, t). \quad (27)$$

3. Numerical Method

The penalized wall function method, proposed in this paper, is implemented in the NOISEtte flow solver [17, 18]. The system of equations (1)–(3), (8) are discretized using vertex-centered finite-volume method, combined with quasi-one-dimensional variable reconstruction along a mesh edge (EBR-scheme) [3], used to increase the order of accuracy. The approximation of the viscous terms is based on Galerkin finite element method with linear basis functions. For time integration, an implicit three-layer 2nd order time integration method is used. At each stage of the time integration the spatially discretized system of nonlinear equations is solved using Newton’s method with the linearized space-difference system of equations at each Newton’s iteration solved using stabilized bi-conjugate gradient method (BI-CGSTAB) [34].

Each time integration step of the main system of equations (1)–(3), (8) is preceded by an implicit first-order time integration of Eq. (25), which for efficiency is discretized using first-order upwind-biased finite-difference method. The Gaussian function (23) is used for the localized

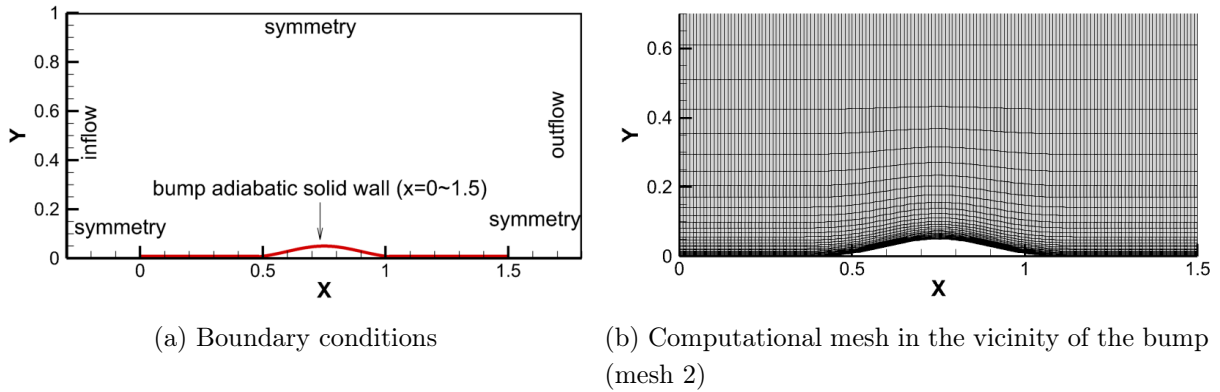


Figure 1. 2D Bump-in-channel flow problem

exchange layer masking function. The values of the normalized thickness of the exchange layer σ^+ , the length scale l_s , the relaxation parameters η_f and η_s , and the initial value of u_τ used in the simulation are discussed in Section 4.

4. Simulations and Results

4.1. 2D Bump-in-channel Flow

To demonstrate the effectiveness and accuracy of the proposed approach, the penalized wall function method is applied for the two dimensional simulation of compressible turbulent flow around a bump, also known as 2D bump-in-channel flow. The flow configuration is identical to the NASA turbulence model verification case [1]. The simulation results are compared with the reference solution [1], obtained using the CFL3D structured grid code [29] with the Spalart–Allmaras model [31].

The problem is non-dimensionalized identically to the reference case [1] using the following characteristic scales: the density of the undisturbed flow ρ_∞ , the inflow velocity U_∞ , the molecular viscosity at the inflow μ_∞ , and the unit length L . The 2D bump-in-channel flow problem is solved for the Reynolds number $Re = 3 \times 10^6$ and the Mach number $M = 0.2$. A viscous compressible flow around an infinitely thin plate with an origin at the point $(0, 0)$ and a dimensionless length of 1.5 with the bump of the height of 0.05 is considered. The geometry of the bump is described as

$$y = \begin{cases} 0.05 \left\{ \sin \left(\frac{\pi x}{0.9} - \frac{\pi}{3} \right) \right\}^4 & \text{if } 0.3 < x < 1.2, \\ 0 & \text{if } x \leq 0.3 \text{ and } x \geq 1.2. \end{cases} \quad (28)$$

The problem set up and the boundary conditions are shown in Fig. 1a. The boundary conditions are as follows. No-slip, adiabatic, zero eddy viscosity condition (12) are imposed at the solid plate surfaces for the RANS simulations using Spalart–Allmaras model [31]. For the penalized wall function method the no-slip and zero eddy viscosity conditions are replaced by no-penetration condition (18), wall shear stress condition (19), and condition (21) for the eddy viscosity.

The penalized wall function method is implemented as follows: the friction velocity field u_τ is defined in the entire computational domain with initial value of $u_\tau = 4 \times 10^{-2}$. The PWF equation (25) is integrated as a preprocessing step before each time integration step of the main

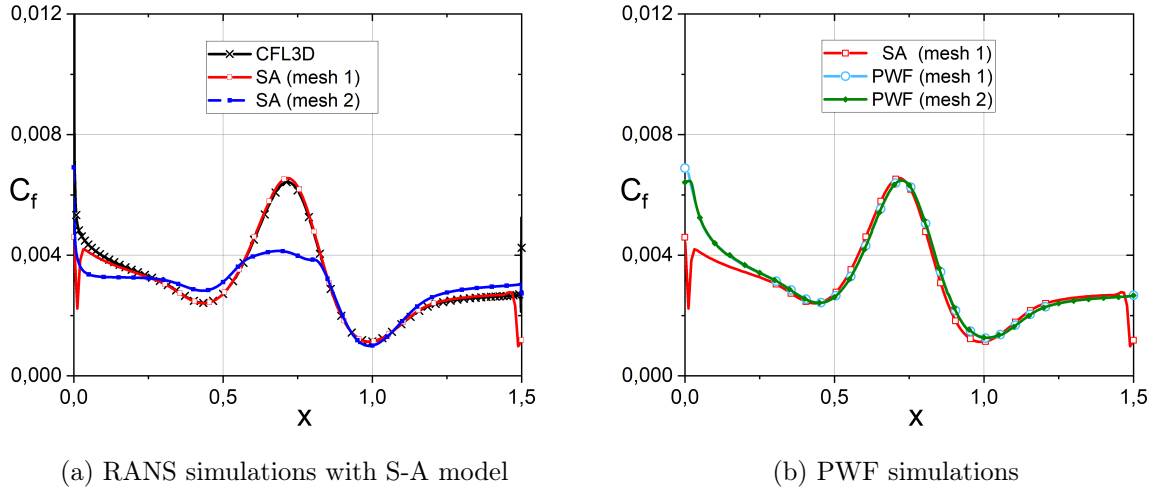


Figure 2. Distribution of the skin friction coefficient on the bump for two different resolutions

system of RANS equations (1)–(3), (8). The updated values of u_τ are subsequently used in the boundary condition (19) and the distance function definition (20) when solving the RANS equations for the next time step. The PWF equation (25) is solved for the localized exchange layer masking function χ_s defined as the Gaussian function (23) with the normalized exchange layer thickness $\sigma^+ = 50$, the normalized distance at the exchange location is $\delta_{EL}^+ = 100$, the nondimensional characteristic length scale $l_s = 1$ and time scales $\eta_s = 10^{-2}$ and $\eta_f = 10^{-2}$, and the Reichardt’s law of the wall [28] for the wall function:

$$f_{\text{Rei}}(y^+) = \frac{1}{\kappa} \ln(1 + \kappa y^+) + 7.8 \left[1 - \exp\left(-\frac{y^+}{11}\right) - \frac{y^+}{11} \exp\left(-\frac{y^+}{3}\right) \right], \quad (29)$$

where $\kappa = 0.41$ is the von Kármán constant.

The simulations are carried out on structured meshes with the longitudinal grid size $\Delta h_{\parallel} \approx 10^{-2}$, which ensures the adequate resolution of the bump curvature. The wall normal mesh size is exponentially increasing with the growth factor of $q \approx 1.2$ and mesh resolution in the vicinity of the wall Δh_{\perp} .

To demonstrate the convergence of the PWF method, the simulations are carried out for two different near-wall resolutions: $\Delta h_{\perp} = 1 \times 10^{-5}$ and $\Delta h_{\perp} = 1 \times 10^{-4}$.

The mesh resolutions are chosen so that the RANS simulations with S-A model are well resolved for the first case, denoted as mesh 1, and unresolved for the second case, denoted as mesh 2. The zoomed-in view of the computational mesh in the vicinity of the bump, corresponding to the unresolved case, is shown in Fig. 1b, where for better visual perception every tenth vertical line is shown.

The results of the PWF simulations are compared with the reference solution [1] and with the results of the RANS simulations with the Spalart–Allmaras model [31], which are carried out on the same computational meshes using the same solver, but with no-slip and zero eddy viscosity (12) boundary conditions instead of the no-penetration condition (18), wall shear stress condition (19), and condition (21) used in the PWF method.

The effect of the wall model is demonstrated in Fig. 2, where skin friction coefficient C_f distribution on the bump for two different resolutions is shown for both the RANS and PWF simulations. As can be seen in Fig. 2a, the results of the resolved RANS simulations are in good

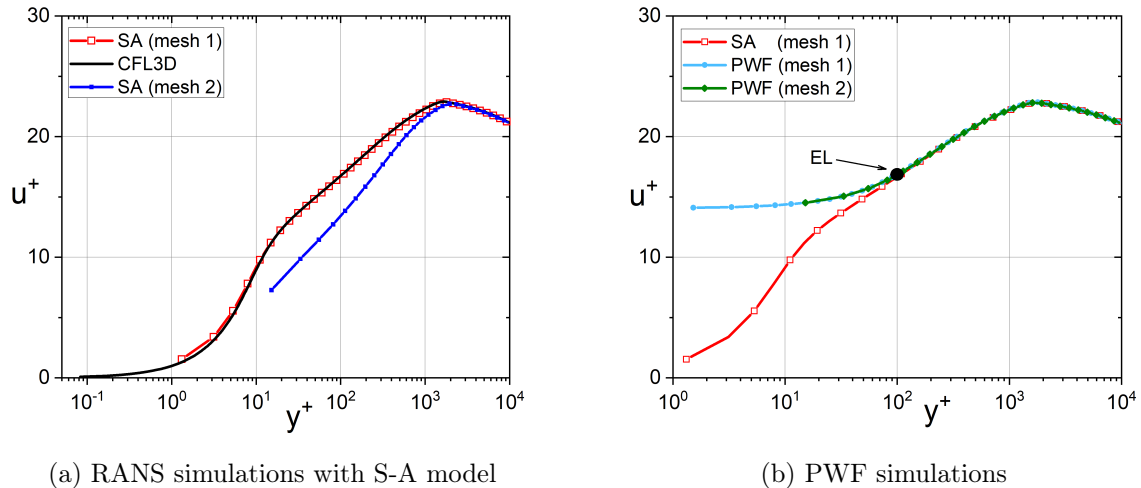


Figure 3. Streamwise velocity profiles at $x = 0.75$ for the 2D bump-in-channel flow problem for two different resolutions

agreement with the reference CFL3D solution [1], while for the second case the skin friction coefficient is significantly underestimated due to insufficient resolution of the boundary layer, required by the S-A model. In contrast, as can be seen in Fig. 2b, the skin friction coefficient distributions for the PWF simulations are practically identical for both resolutions and are in good agreement with the results of the resolved RANS simulations, which highlights the substantially lower near wall resolution requirements for the penalized wall function method compared to the resolved RANS simulations with S-A turbulence model. Note that the deviations of the skin friction coefficient at the leading and trailing edges of the plate are related to geometric singularities caused by the sudden application of either no-slip or wall shear stress conditions on the plate for the RANS and PWF simulations, respectively.

A similar trend is observed when considering velocity profiles. A comparison of the streamwise velocity profiles in the wall-normal direction at $x = 0.75$ is given in Figs. 3a and 3b, where the results of the RANS and PWF simulations, respectively, are shown. As can be seen in Fig. 3a the resolved RANS simulations with S-A model are in good agreement with the reference CFL3D solution [1], while for the unresolved case (mesh 2) the velocity profile is wrong. Substantially lower wall resolution requirements of the PWF method are demonstrated in Fig. 3b, which shows good agreement between the results of PWF simulations for all resolutions both in the boundary layer and in the outer region. Moreover, as can be seen in Fig. 3b, the PWF solution in the outer region, marked by the exchange location, is in excellent agreement with the results of the resolved RANS simulation with S-A turbulence model.

The distribution of relative turbulent viscosity $\nu_T^+ = \nu_T/\nu$ in the wall-normal direction at $x = 0.75$ is shown in Figs. 4a and 4b for RANS and PWF simulations, respectively. As can be seen in Fig. 4a the value of turbulence viscosity is substantially higher for the unresolved case, compensating for the lack of wall normal resolution. The results of the resolved RANS simulations with the S-A turbulence model are slightly higher than the reference CFL3D solution [1], which is due to slightly lower resolution compared to the reference case. The eddy-viscosity for the PWF simulations for both resolutions are identical and in the outer region ($y^+ > \delta_{EL}^+$) are slightly lower compared to the eddy-viscosity of the resolved RANS simulation with the S-A turbulence

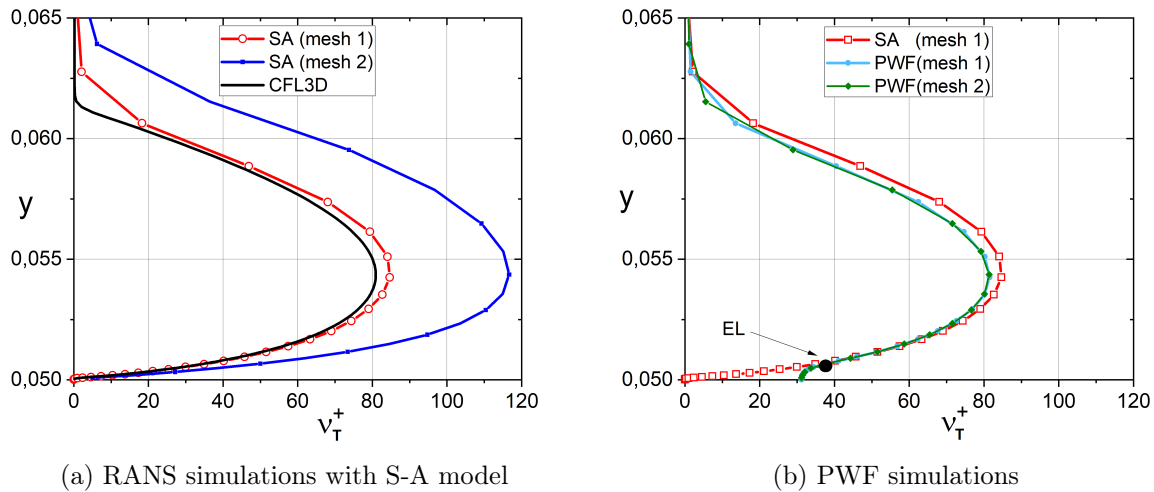


Figure 4. Eddy-viscosity profiles at $x = 0.75$ for the 2D bump-in-channel flow problem for two different resolutions

model. This discrepancy is related to limiting the wall distance according to Eq. (20), which, in turn, results in almost constant eddy-viscosity in the inner region ($y^+ < \delta_{EL}^+$).

Conclusions

A novel penalized wall function method is proposed for simulations of wall-bounded compressible turbulent flows. The new approach, similar to classical wall function methods, is based on the Reynolds-averaged Navier–Stokes (RANS) equations to model the outer region of the turbulent boundary layer, while approximating the inner part by an analytic wall function. The differential formulation to match the outer and wall function solutions is reformulated in a form of a generalized characteristic-based volume penalization method for the friction velocity to model the transfer of the shear stress from the outer region of the boundary layer to the wall and to impose the wall-stress boundary conditions on the RANS solution. The exchange location in the new formulation is specified implicitly through a localized source term in the boundary layer equation, which eliminates the need to interpolate the solution to the exchange location as well as the need to explicitly determine the position of the exchange location. The wall-stress condition is determined by solving an auxiliary equation for the friction velocity, ensuring the correct matching of the RANS and the wall function solutions at the exchange layer. The penalized wall function method is demonstrated for Reynolds-averaged Navier–Stokes equations with the Spalart–Allmaras turbulence model, but can be used in conjunction with any turbulence model that allows transfer of shear stress from the outer region of the boundary layer to the wall.

The proposed method noticeably reduces the near-wall mesh resolution requirements without significant modification of the RANS solver. The formulation of the penalized wall function method is general and can be used in context of any numerical method based on either structured or unstructured meshes.

The effectiveness of the developed penalized wall function method is demonstrated for two-dimensional bump-in-channel flow, which is characterized by the presence of a significant longitudinal pressure gradient without flow separation. The simulations demonstrate the sufficient accuracy of the PWF solution on grids with 10 times coarser near wall resolution compared to the resolution required by the the Spalart–Alamaras model with no-slip boundary conditions.

Further development of PWF method includes its generalization to problems with strong pressure gradients and flow separation, which would require the reformulation of the method in terms of differential equilibrium and non-equilibrium wall functions.

Acknowledgements

This work has been carried out using computing resources of the federal collective usage center Complex for Simulation and Data Processing for Mega-science Facilities at NRC “Kurchatov Institute”, <http://ckp.nrcki.ru/>.

References

1. NASA Langley research center turbulence modeling resource, <https://turbmodels.larc.nasa.gov>, accessed: 2022-11-07
2. Abalakin, I.V., Vasilyev, O.V., Zhdanova, N.S., Kozubskaya, T.K.: Characteristic based volume penalization method for numerical simulation of compressible flows on unstructured meshes. *Comput. Math. and Math. Phys.* 61(8), 1315–1329 (2021). <https://doi.org/10.1134/S0965542521080029>
3. Bakhvalov, P., Abalakin, I., Kozubskaya, T.: Edge-based reconstruction schemes for unstructured tetrahedral meshes. *Int. J. Numer. Meth. Fluids* 81(6), 331–356 (2016). <https://doi.org/10.1002/flid.4187>
4. Bardina, J., Huang, P., Coakley, T., *et al.*: Turbulence modeling validation. In: 28th Fluid dynamics conference. p. 2121 (1997)
5. Beaugendre, H., Morency, F.: Penalization of the Spalart–Allmaras turbulence model without and with a wall function: Methodology for a vortex in cell scheme. *Computers & Fluids* 170, 313–323 (Jul 2018), <https://hal.inria.fr/hal-01963687>
6. Beaugendre, H., Morency, F.: Penalization of the Spalart–Allmaras turbulence model without and with a wall function: Methodology for a vortex in cell scheme. *Computers & Fluids* 170, 313–323 (2018). <https://doi.org/10.1016/j.compfluid.2018.05.012>
7. Bodart, J., Larsson, J.: Wall-modeled large eddy simulation in complex geometries with application to high-lift devices. *Annual Research Briefs, Center for Turbulence Research, Stanford University* pp. 37–48 (2011)
8. Brown-Dymkoski, E., Kasimov, N., Vasilyev, O.V.: A characteristic based volume penalization method for general evolution problems applied to compressible viscous flows. *J. Comp. Phys.* 262, 344–357 (2014). <https://doi.org/10.1063/1.4825260>
9. Brown-Dymkoski, E., Kasimov, N., Vasilyev, O.V.: A characteristic-based volume penalization method for arbitrary mach flows around solid obstacles. In: Fröhlich, J., Kuerten, H., Geurts, B.J., Armenio, V. (eds.) *Direct and Large-Eddy Simulation IX*. pp. 109–115. Springer, Cham (2015). https://doi.org/10.1007/978-3-319-14448-1_15
10. Cai, S.G., Degryny, J., Boussuge, J.F., Sagaut, P.: Coupling of turbulence wall models and immersed boundaries on cartesian grids. *J. Comp. Phys.* 429, 109995 (2021). <https://doi.org/10.1016/j.jcp.2020.109995>

11. Craft, T., Gant, S., Gerasimov, A., *et al.*: Development and application of wall-function treatments for turbulent forced and mixed convection flows. *Fluid Dyn. Res.* 38(2), 127–144 (2006). <https://doi.org/10.1016/j.fluiddyn.2004.11.002>
12. Dhamankar, N., Blaisdell, G., Lyrintzis, A.: Implementation of a wall-modeled sharp immersed boundary method in a high-order large eddy simulation tool for jet aeroacoustics. In: 54th AIAA Aerospace Sciences Meeting (01 2016). <https://doi.org/10.2514/6.2016-0257>
13. Duben, A.P., Abalakin, I.V., Tsvetkova, V.O.: On boundary conditions on solid walls in viscous flow problems. *Math. Models and Comput. Simul.* 13(4), 591–603 (2021). <https://doi.org/10.1134/S2070048221040128>
14. Durbin, P.A., Reif, B.A.P.: *Statistical Theory and Modeling for Turbulent Flows*. Wiley (2001)
15. Froehlich, J., von Terzi, D.: Hybrid LES/RANS methods for the simulation of turbulent flows. *Progress in Aerospace Sciences* 44(5), 349–377 (2008). <https://doi.org/10.1016/j.paerosci.2008.05.001>
16. Gatski, T.B., Hussaini, M.Y., Lumley, J.L.: *Simulation and Modeling of Turbulent Flows*. Oxford (1996)
17. Gorobets, A., Bakhvalov, P.: Heterogeneous CPU+GPU parallelization for high-accuracy scale-resolving simulations of compressible turbulent flows on hybrid supercomputers. *Comput. Phys. Commun.* 271, 108231 (2022). <https://doi.org/10.1016/j.cpc.2021.108231>
18. Gorobets, A., Duben, A.: Technology for supercomputer simulation of turbulent flows in the good new days of exascale computing. *Supercomput. Front. Innov.* 8(4), 4–10 (Feb 2021). <https://doi.org/10.14529/jsfi210401>
19. Kasimov, N., Dymkoski, E., De Stefano, G., Vasilyev, O.V.: Galilean-invariant characteristic-based volume penalization method for supersonic flows with moving boundaries. *Fluids* 6(8) (2021). <https://doi.org/10.3390/fluids6080293>
20. Kawai, S., Larsson, J.: Wall-modeling in large eddy simulation: length scales, grid resolution, and accuracy. *Phys. Fluids.* 24(1), 015105 (2012). <https://doi.org/10.1063/1.3678331>
21. Kawai, S., Larsson, J.: Dynamic non-equilibrium wall-modeling for large eddy simulation at high Reynolds numbers. *Phys. Fluids.* 25(1), 015105 (2013). <https://doi.org/10.1063/1.4775363>
22. Liu, Q., Vasilyev, O.V.: Hybrid adaptive wavelet collocation – Brinkman penalization method for unsteady RANS simulations of compressible flow around bluff bodies. In: 36th AIAA Fluid Dynamics Conference and Exhibit, San Francisco, California, USA, June 5–8, 2006 (2006). <https://doi.org/10.2514/6.2006-3206>
23. Liu, Q., Vasilyev, O.V.: A Brinkman penalization method for compressible flows in complex geometries. *J. Comp. Phys.* 227(2), 946–966 (2007). <https://doi.org/10.1016/j.jcp.2007.07.037>
24. Moin, P., Mahesh, K.: Direct numerical simulation: A tool in turbulence research. *Annual Rev. Fluid Mech.* 30, 539–578 (1998). <https://doi.org/10.1146/annurev.fluid.30.1.539>

25. Nichols, R.H., Nelson, C.C.: Wall function boundary conditions including heat transfer and compressibility. *AIAA Journal* 42(6), 1107–1114 (2004). <https://doi.org/10.2514/1.3539>
26. Park, G.I., Moin, P.: An improved dynamic non-equilibrium wall-model for large eddy simulation. *Phys. Fluids*. 26(1), 37–48 (2014). <https://doi.org/10.1063/1.4861069>
27. Patankar, S.V., Spalding, D.B.: *Heat and Mass Transfer in Boundary Layers*. Morgan-Grampia (1968)
28. Reichardt, H.: Vollständige darstellung der turbulenten geschwindigkeitsverteilung in glatten leitungen. *Zeitschrift für Angewandte Mathematik und Mechanik* 31(7), 208–219 (1951)
29. Rumsey, C., Gatski, T., Sellers, W., *et al.*: Summary of the 2004 CFD validation workshop on synthetic jets and turbulent separation control. In: 2nd AIAA Flow Control Conference, Portland, Oregon, June 28 – July 1, 2004. p. 2217 (2004). <https://doi.org/10.2514/6.2004-2217>
30. Shur, M.L., Spalart, P.R., Strelets, M.K., Travin, A.K.: A hybrid RANS-LES approach with delayed-DES and wall-modelled LES capabilities. *Int. J. Heat Fluid Flow* 29(6), 1638–1649 (2008). <https://doi.org/10.1016/j.ijheatfluidflow.2008.07.001>
31. Spalart, P.R., Allmaras, S.R.: A one equation turbulence model for aerodynamic flows. *AIAA journal* 94 (1992). <https://doi.org/10.2514/6.1992-439>
32. Spalart, P.R., Deck, S., Shur, M.L., *et al.*: A new version of detached-eddy simulation, resistant to ambiguous grid densities. *Theoretical and computational fluid dynamics* 20(3), 181–195 (2006). <https://doi.org/10.1007/s00162-006-0015-0>
33. Spalart, P.R., Jou, W.H., Strelets, M., *et al.*: Comments on the feasibility of LES for wings, and on a hybrid RANS/LES approach. In: First AFOSR international conference on DNS/LES, Ruston, Louisiana. vol. 1, pp. 4–8. Greyden Press, Columbus, OH (1997)
34. van der Vorst, H.A.: BI-CGSTAB: A fast and smoothly converging variant of BI-CG for the solution of nonsymmetric linear systems. *SIAM J. Sci. Stat. Comput.* 13(2), 631–644 (1992). <https://doi.org/10.1137/0913035>
35. Wilcox, D.C.: Formulation of the $k - \omega$ turbulence model revisited. *AIAA Journal* 46(11), 2823–2838 (2008). <https://doi.org/10.2514/1.36541>
36. Xiao, H., Jenny, P.: A consistent dual-mesh framework for hybrid LES/RANS modeling. *J. Comp. Phys.* 231(4), 1848–1865 (FEB 20 2012). <https://doi.org/10.1016/j.jcp.2011.11.009>
37. Zhdanova, N.S., Abalakin, I.V., Vasilyev, O.V.: Generalized Brinkman volume penalization method for compressible flows around moving obstacles. *Math. Models. and Comput. Simul.* 14(5), 716–726 (2022). <https://doi.org/10.1134/S2070048222050180>